Atomic masses of ^{32,33}S, ^{84,86}Kr, and ^{129,132}Xe with uncertainties ≤0.1 ppb

Wei Shi, Matthew Redshaw, and Edmund G. Myers
Department of Physics, Florida State University, Tallahassee, Florida 32306-4350, USA
(Received 30 March 2005; published 19 August 2005)

The atomic masses of ^{32}S, ^{84,86}Kr, and ^{129,132}Xe have been measured by comparing cyclotron frequencies of single ions in a Penning trap. The results (with one standard deviation uncertainties) are $M(^{32}\mathrm{S})=31.972\,071\,173\,5(16)$, $M(^{84}\mathrm{Kr})=83.911\,497\,770\,5(50)$, $M(^{86}\mathrm{Kr})=85.910\,610\,672\,2(84)$, $M(^{129}\mathrm{Xe})=128.904\,780\,960(10)$, and $M(^{132}\mathrm{Xe})=131.904\,155\,190\,7(92)$. Combining our mass of ^{32}S with the high-precision mass difference between $^{33}\mathrm{S}^+$ and $^{32}\mathrm{SH}^+$ obtained by Rainville *et al.* [submitted to Nature], we also obtain $M(^{33}\mathrm{S})=32.971\,458\,908\,7(16)$. These results are more precise than previous data by factors of 13 to 600.

DOI: 10.1103/PhysRevA.72.022510 PACS number(s): 32.10.Bi, 06.20.Jr, 07.75.+h, 82.80.Qx

I. INTRODUCTION

The development of single-ion Penning trap techniques in the 1980s enabled the first atomic mass measurements at better than 1 ppb precision [1,2]. Refinement of these techniques has now led to a comparison of the mass of the proton and anti-proton at 0.1 ppb by the Harvard group [3], and mass measurements of ^{16}O and ^{4}He at 10 and 16 ppt, respectively, by the Washington group [4,5]. For other atoms with $A>4$, the highest precision measurements have been carried out at MIT. These include sub-0.1 ppb measurements of ^{13}C, ^{14,15}N, ^{28}Si, ^{40}Ar; and sub-0.2 ppb measurements of ^{20}Ne and the alkali metals ^{23}Na, ^{85,87}Rb, and ^{133}Cs [6,7]. As their final work the MIT group developed a technique for simultaneous cyclotron frequency measurement on two ions in the same trap. This yielded the mass ratios $^{14}\mathrm{N_2}^+/^{13}\mathrm{C_2H_2}^+$ [8], $^{14}\mathrm{N_2}^+/\mathrm{CO}^+$ [9], $^{29}\mathrm{Si}^+/^{28}\mathrm{SiH}^+$, and $^{33}\mathrm{S}^+/^{32}\mathrm{SH}^+$ [10] at 7 to 15 ppt precision. After this the present authors took charge of the MIT apparatus and moved it to its new location at Florida State University.

After rebuilding the apparatus in Tallahassee, we decided that the first atomic mass measurements should use single-ion techniques and aim for 0.1 ppb precision. We chose to measure the atomic mass of ^{32}S so that, combined with the $^{33}\mathrm{S}^+/^{32}\mathrm{SH}^+$ result of [10], two more isotopes could be added to the precision atomic mass table of elements with $Z\leqslant 18$ [11]; ^{84,86}Kr with isotopic abundances of 57.0% and 17.3%, and ^{129,132}Xe with abundances of 26.4% and 26.9%, are the two most abundant isotopes of the two heaviest stable rare gases. These measurements should provide convenient calibrations for mass spectrometers in diverse fields including nuclear physics and chemistry. They may also have future application to metrology, tests of physical laws, and determination of fundamental constants.

While our measurement of the mass of ^{32}S was relatively straightforward, the setup and our procedures were not fully optimized for the heavier mass isotopes which involved measurements at relatively high values of mass-to-charge ratio of 40 to 44. This required significant corrections to be made to the measured mass ratios. Nevertheless, by modeling these systematic effects and carrying out the necessary auxiliary measurements, we believe we have accounted for them at a level consistent with sub-0.1 ppb precision. As a by-product, we have made explicit some details of the single-ion mass measurement techniques developed at MIT that have not been discussed previously.

II. EXPERIMENT

Details of the MIT mass spectrometer and procedures, the majority of which we followed, can be found in Refs. [12–15]. Here we give only a brief description. Many of the principles and the standard terminology of single-ion Penning trap physics are given in Ref. [16].

A. The Penning trap

The Penning trap consists of a ring and two end-cap electrodes, with hyperbolic inner surfaces, and characteristic dimension $d=5.5$ mm, immersed in a 8.5 T magnetic field. Positive ions are trapped axially by biasing the ring negative with respect to the end-caps. Additional "guard-ring" electrodes are placed between the ring and each end-cap. The guard-ring voltage can be adjusted to reduce the lowest-order electrostatic field imperfection, quantified by the C_4 parameter. The upper end-cap has a 0.5 mm diameter hole for admitting gas molecules, while the lower end-cap has a similar hole for admitting the electron beam that is used to make the ions. The trap electrodes are made of copper with alumina spacers and are mounted inside a copper vacuum can. This forms the lower end of a 1.75 m cryogenic "insert" located in the vertical bore of a superconducting NMR magnet (Oxford Instruments 360-89). Ultrahigh vacuum is produced in the can by filling the surrounding bore with liquid helium, enabling ions to be trapped for several days. Prior to installing the insert, a helically scanned NMR probe was used to map the magnetic field. After shimming to produce a uniform field, the linear and quadratic axial field gradients were measured to be $|B_1/B_0|<4\times10^{-9}$ mm^{-1} and $|B_2/B_0|<1.5\times10^{-10}$ mm^{-2}, respectively.

The voltage applied to the ring is derived from a stable precision voltage source under computer control. This voltage is periodically adjusted to bring the ion's axial frequency into resonance with a superconducting coil at 4.2 K, which is

connected across the end-caps. During our experiment the coil Q was typically 33 000 and its resonant frequency 213 kHz. The image current induced by the ion's axial motion results in a back EMF from the coil that damps the axial motion, and, by coupling of the coil to a dc superconducting quantum interference device (SQUID), provides our only signal. The axial motion has been shown to damp to the 4.2 K temperature of the coil [14]. The damping time constant for the ion's axial energy [see Eq. (7) below], was typically 1 to 2 s.

B. Ion making

Ions are produced in the trap by admitting a carefully metered quantity of gas, typically 10^{-2} torr cm^3, into the top of the insert. From here to the top of the trap there is a clear line-of-sight formed by a series of 5 mm diameter apertures located along the bore of the insert. Most of the gas is cryopumped along this bore: the residual forms a molecular beam which is incident on the 0.5 mm diameter aperture in the upper end-cap. For 1 to 5 s, simultaneous with gas injection, a field-emission point below the lower end-cap emits a 5–20 nA, ~750 eV electron beam that passes upwards through the lower end-cap. Trapped ions are produced by electron impact ionization of gas molecules as they pass through the trap. After each attempt at making an ion of the desired species, a sequence of procedures is used to cool the ion to the center of the trap and eliminate all other ions. Briefly, the desired ion is cooled to the trap center by scanning the ring voltage to bring the ion to resonance with the coil, allowing for frequency shifts due to other ions and due to trap anharmonicity. The undesired ions are then removed by selectively exciting their axial motion using various rf drives, and then lowering the potential on the lower end-cap until they collide with it and are lost.

That we have isolated a single ion of the correct species is determined from the width and stability of the Fast-Fourier transform of the axial ring-down signal after the ion is excited by a rf pulse applied to the lower end-cap. Depending on the relative abundance of the desired ion in the ion cloud—the extremes were N_2^+ and $^{129,132}Xe^{3+}$—it required 5 to 30 min to produce and isolate the ion. The gases used all had natural isotopic abundances. These procedures and all the experimental control and data taking were greatly facilitated by an extensive computerized control system [14,15].

C. Reference ions

To obtain the mass of ^{32}S we compared $^{32}S^+$ (made from H_2S), to the mass-32 ions $^{16}O_2^+$ and $^{12}C_2D_4^+$ (from C_2D_4). As will be seen later, the use of "mass-doublets" avoids several sources of systematic error. The mass of ^2D has been determined to a fractional precision of 1.8×10^{-10} [11], so that $^{12}C_2D_4^+$ is known to 4.5×10^{-11}. For ^{84}Kr the main reference was $^{14}N_2^+$, which was compared to $^{84}Kr^{3+}$ at $m/q=28$. Combining the recent MIT ratio of $^{14}N_2^+/^{12}C^{16}O^+$ [9], with the value for $M(^{16}O)$ from Ref. [4], gives $M(^{14}N)$ to 1.6×10^{-11}. We also measured $^{84}Kr^{2+}$ against $^{40}Ar^+$ and CO_2^+; the mass of ^{40}Ar has been determined to 7×10^{-11} [11]. The masses of ^{86}Kr and $^{129,132}Xe$ were then obtained by comparing each of $^{86}Kr^{2+}$, $^{129}Xe^{3+}$, and $^{132}Xe^{3+}$ to both $^{84}Kr^{2+}$ and CO_2^+. We note that $^{132}Xe^{3+}$ is a doublet with CO_2^+, while $^{86}Kr^{2+}$ and $^{129}Xe^{3+}$ lie midway between $^{84}Kr^{2+}$ and CO_2^+. For improved statistical precision and to provide consistency checks, we also measured all ratios among $^{86}Kr^{2+}$, $^{129}Xe^{3+}$, and $^{132}Xe^{3+}$. Initially we attempted to use $^{12}C_3H_6^+$ (made from propylene) as a reference for mass-42. However, we found that this ion's cyclotron frequency sometimes exhibited jumps at the level of several 10^{-9} during a run. We speculate this was due to large, rotational state-dependent variations in the polarizability, which affect the cyclotron frequency, as discussed in Ref. [9]. By contrast, the symmetries of $^{14}N_2^+$, $^{16}O_2^+$, $^{12}C^{16}O_2^+$, and $^{12}C_2D_4^+$ are such that they have negligible body-frame electric dipole moments, and are not expected to show significant shifts in cyclotron frequency due to polarization.

D. Obtaining the cyclotron frequency

In principle, one obtains the mass ratio of a pair of ions from the ratio of their cyclotron frequencies, $f_c=(1/2\pi)qB/m$, where B is the magnetic field, and q and m are the charge and mass of the ion, respectively. However, the trap electrostatic field reduces the cyclotron frequency to the "trap-cyclotron frequency" f_{ct}, and also causes the guiding center of the cyclotron motion to precess about the electrostatic center of the trap at the magnetron frequency, f_m. The cyclotron frequency we require, i.e., that which would occur in the absence of the electrostatic field, can be obtained using the "invariance theorem," $f_c^2=f_{ct}^2+f_z^2+f_m^2$, which relates f_c to the measurable trap-cyclotron, axial, and magnetron frequencies. As shown in Ref. [16], this relation is valid, except for relativistic corrections, provided only the magnetic field is uniform and the electrostatic potential is quadratic, i.e., it allows for the electrostatic field axis to be tilted with respect to the magnetic field and also for the electrostatic field to be ellipsoidal.

We measured f_{ct}, which was in the range 2.9 to 4.6 MHz, using the so-called "pulse and phase" (PNP) technique [1]. In this procedure the cyclotron and magnetron motions are first cooled by applying rf voltages at the "coupling" frequencies $f_{cc}=f_{ct}-f_z$, and $f_{mc}=f_m+f_z$, to one-half of one of the guard-ring electrodes (the guard-ring electrodes are divided into two halves). This produces a "tilted" quadrupole rf electrostatic field component which couples the respective radial mode to the axial mode [17]. After this initialization, the ion is then driven into a cyclotron orbit of well-defined radius, 170 to 200 μm, with well-defined initial phase, by applying a rf voltage within 0.5 Hz of f_{ct} to the guard-ring half, for an interval of typically 25 to 45 ms. The rf field at the ion also has a horizontal dipole component: for sufficiently short drive times the cyclotron radius is proportional to the drive time. The cyclotron motion is then allowed to evolve, without any driving fields or damping, for a definite "phase evolution time" t_{evol}. At the end of this period, a pulse at the cyclotron coupling frequency f_{cc}, and optimally chosen duration (i.e., a "pi-pulse"), is used to transfer the cyclotron motion into a phase-coherent axial motion. This is damped

and detected by the coil and the SQUID. Hence, except for various phase offsets, the final phase of the cyclotron motion ϕ_{ct} is obtained from the phase of the resulting axial ring-down signal, which is mixed-down to near 250 Hz and digitized. The trap cyclotron frequency $f_{ct}=(1/2\pi)d\phi_{ct}/dt_{evol}$, is obtained by repeating the procedure with different t_{evol}'s. We used a sequence of 10 PNP's with t_{evol}'s ranging from 0.1 to 60 sec, which we call a "PNP cycle." Most precision is derived from the longest and shortest t_{evol}'s. However, the intermediate times are required to unambiguously "phase-unwrap," i.e., to assign the correct whole number of 2π's to each measured phase, starting from an initial estimate of f_{ct}, which we obtain using the "avoided-crossing method" [17]. Including the necessary cooling time, a single measurement of f_{ct} required 5 to 10 min and gave a precision of 2 to 3 $\times 10^{-10}$.

The axial signal at the end of each PNP also produces an estimate of the ion's axial frequency f_z. These were averaged over the 10 PNP's of a cycle to produce a $\langle f_z \rangle$ that we associate with the value of f_{ct} from the cycle. To obtain the corresponding magnetron frequency, we made use of the approximate relation [16] $f_m=(f_z^2/2f_{ct})[1+(9/4)\sin^2\theta_{mag}]$, where $\sin^2\theta_{mag}$ is used to parametrize the effects of both trap tilt and ellipticity. By measuring f_m at the beginning of each run we obtained θ_{mag}, and hence could obtain f_m with sufficient precision for each PNP cycle from the measured values of f_z and f_{ct}. We found $\theta_{mag}=0.59(1)$ deg, stable throughout the experiment.

E. Data-taking procedure

Our superconducting magnet, although we pressure-stabilize the helium bath, still exhibits random variations in field of $\sim 10^{-9}$/h superimposed on a slower long-term decay. Our mass-comparison procedure was hence to make and isolate the first ion in the trap, measure its cyclotron frequency, then replace it with the other ion, etc., and interchange as frequently as practical. Since it took up to 30 min to make the more difficult ions, we adopted the procedure of repeating each PNP cycle three times, which took 20 to 30 min, before ejecting the ion and making the other. In this way we obtained between 5 and 7 "ion pairs" in an 8 to 10 h run. Each run generally gave a statistical precision for determining a cyclotron frequency ratio of $\sim 10^{-10}$. The daytime ambient magnetic field in our underground laboratory, as recorded with a flux-gate magnetometer, generally varied by <0.2 mG/h, while the shielding factor of our superconducting magnet is greater than 7. We found that variations in magnetic field due to internal changes of the magnet usually dominated variation due to the ambient field. We recorded the ambient field throughout the run but found no overall improvement in precision by correcting for it, nor did we obtain significant improvement by taking data at night.

F. Cyclotron frequency ratio data

Figure 1 shows the cyclotron frequencies from one run used to measure the mass ratio of $^{32}S^+$ to $^{16}O_2{}^+$ (all the other runs have a similar appearance). Each point represents a measurement of f_c obtained from the 10-PNP cycle as discussed above, plotted against time during the run. To extract a cyclotron frequency ratio, we used a bivariate fitting routine to fit the same polynomial function, but with a constant offset between them, to the f_c's of both ions. (We first scale one ion's f_c to make this difference small.) The information of interest is contained in the best value for the offset, and this is relatively insensitive to the order of the polynomial used to follow the magnetic field variation. Nevertheless, we fit polynomials of order up to 10 and select the optimum order using the F-test [12]. We employed ordinary Gaussian statistics rather than "robust statistics" in these fits. Bad data, such as when noise in the detector causes the determination of the phase from a PNP ring-down to fail, were eliminated previously during the phase-unwrapping procedure. These and other analysis procedures followed work at MIT but were coded and tested at FSU. Figure 2 shows a histogram of the residuals of f_c compared to the best fit, for all the measurements that make up the $^{32}S^+$ data set.

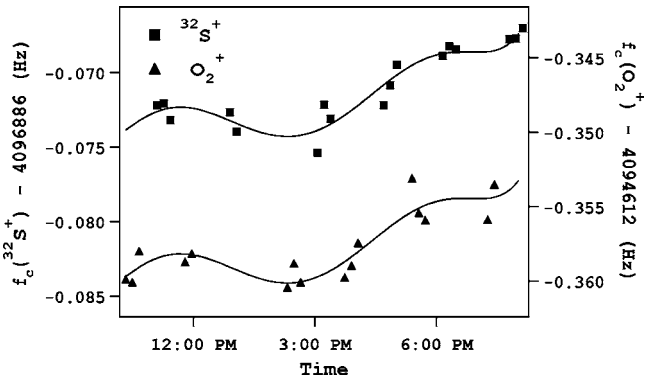

FIG. 1. Typical cyclotron frequency data obtained from one run of $^{32}S^+$ vs $^{16}O_2{}^+$. The curves show the result of a simultaneous fit to a sixth-order polynomial.

The cyclotron frequency ratios, averaged over repeated runs [18], without corrections for systematic effects, see below, are given in the third column of Table I. The statistical uncertainties in these ratios were determined from the uncertainties provided by the routine that produces the simultaneous fits, as in Fig. 1.

III. CORRECTIONS TO THE CYCLOTRON FREQUENCY RATIOS

A. Amplitude-dependent corrections

Deviations in the electrostatic potential from a pure quadrupole, and of the magnetic field from uniformity, and also special relativity, lead to amplitude-dependent shifts in the eigenfrequencies f_{ct}, f_z, and f_m [16], and hence in our derived f_c. It can be shown that the shifts depend on even powers of the amplitudes ρ_c, a_z, ρ_m, and that cylindrical symmetry can be assumed. The electrostatic anharmonicities can hence be expressed in terms of coefficients C_4, C_6, etc., of the Legendre polynomial expansion of the potential, and the magnetic anharmonicities can be expressed in terms of the coefficients B_2, B_4, etc., in the associated Legendre polynomial

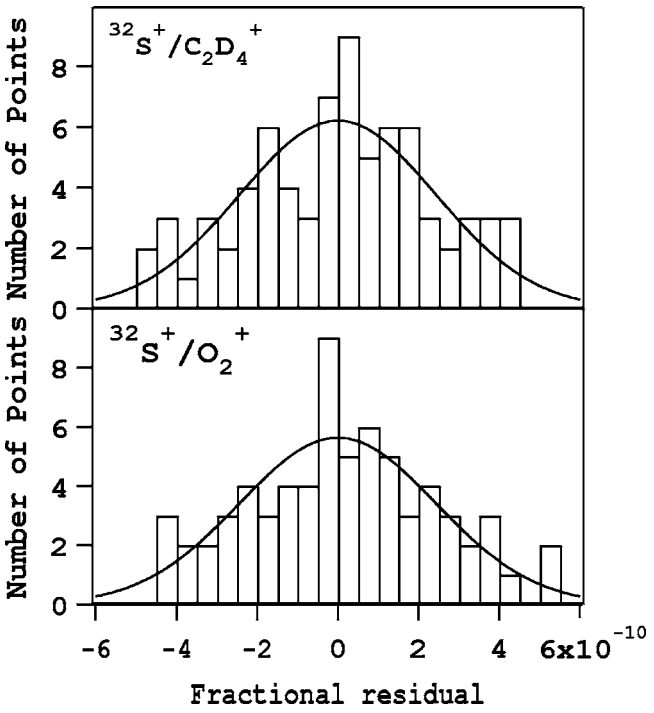

FIG. 2. Histogram of the residuals of the cyclotron frequencies with respect to the simultaneous fit, for all the data used to obtain the mass of ^{32}S. The curves are Gaussian fits. Both sets of data have a standard deviation of 2.5×10^{-10}.

expansion of the field [16]. Expressions including terms up to C_8 and B_4 can be found in Ref. [14].

During the phase evolution period of our f_{ct} measurements, the axial motion is cooled to thermal equilibrium with the coil. This results in a rms "thermal" amplitude of $a_z^{th}=35$ μm at $m/q=32$, scaling as $m^{-1/2}$, but independent of charge. The magnetron motion and cyclotron motion, prior to application of the cyclotron drive pulse, are cooled by "action exchange" with the damped axial motion with the result $\rho_c^{th}=\rho_m^{th}=(f_z/f_{ct})^{1/2}a_z^{th}=8$ μm for $q=1$, scaling as $q^{-1/2}$, but independent of mass. These thermal amplitudes lead to negligible shifts and are small compared to the cyclotron radius during the phase evolution period. Hence, following Refs. [14–16], the shift in the trap cyclotron frequency can be approximated by

$$\frac{\Delta f_{ct}}{f_{ct}}=\left[\frac{3}{2}\frac{f_m}{f_{ct}}\frac{C_4}{d^2}-\frac{1}{2}\frac{B_2}{B_0}-\frac{1}{2}\left(\frac{2\pi f_{ct}}{c}\right)^2\right]\rho_c^2, \tag{1}$$

where the three terms represent the leading contributions from electrostatic and magnetic imperfections, and from special relativity, respectively. Likewise ignoring thermal amplitudes, the shift in our measured axial frequency, obtained from the ring-down after the coupling pulse, is approximated by

$$\frac{\Delta f_z}{f_z}=\left[-\frac{3}{2}\frac{C_4}{d^2}+\frac{1}{4}\frac{f_{ct}}{f_m}\frac{B_2}{B_0}\right]\rho_{c\text{-}res}^2+\frac{\Delta f_z(a_z)}{f_z}, \tag{2}$$

where $\rho_{c\text{-}res}$ is the residual cyclotron radius due to imperfect cyclotron-to-axial action transfer by the coupling pulse, and $\Delta f_z(a_z)$ is the shift in the measured axial frequency due to the axial amplitude a_z at the start of the ring-down. If a_z were constant, $\Delta f_z(a_z)/f_z$ could be expressed as

$$\frac{\Delta f_z(a_z)}{f_z}=\frac{3}{4}\frac{C_4}{d^2}a_z^2+\frac{15}{16}\frac{C_6}{d^4}a_z^4. \tag{3}$$

However, the axial frequency determination is made from the entire ring-down signal in which Δf_z is chirping and the average values of a_z^2 and a_z^4 are considerably reduced. We hence decided it was preferable to measure $\Delta f_z(a_z)$ directly using auxiliary measurements. [The C_6 term is included in Eq. (3) but not Eq. (1) because the axial amplitude at the

TABLE I. Measured cyclotron frequency (inverse mass) ratios. N is the number of runs; R (uncorrected) is the average ratio without correction for systematic effects with uncertainty (in parentheses) obtained from the error provided by the simultaneous fitting routine; Δ_{syst} is the total systematic correction with estimated uncertainty; R (corrected) is our final result for the ratio with combined statistical and systematic uncertainty.

Ion pair	N	R (uncorrected)	Δ_{syst} ($\times10^{-12}$)	R (corrected)
$^{32}S^+/^{16}O_2^+$	3	1.000 555 433 761(59)	−12(18)	1.000 555 433 749(62)
$^{32}S^+/^{12}C_2D_4^+$	3	1.002 637 844 685(58)	29(10)	1.002 637 844 714(59)
$^{14}N_2^+/^{84}Kr^{3+}$	4	0.998 727 085 572(59)	−26(32)	0.998 727 085 546(67)
$^{84}Kr^{2+}/^{40}Ar^+$	3	0.952 488 231 114(63)	369(160)	0.952 488 231 483(172)
$^{84}Kr^{2+}/^{12}C^{16}O_2^+$	3	1.048 482 198 509(88)	−579(214)	1.048 482 197 930(231)
$^{86}Kr^{2+}/^{84}Kr^{2+}$	3	0.976 730 017 252(49)	17(137)	0.976 730 017 268(146)
$^{86}Kr^{2+}/^{12}C^{16}O_2^+$	3	1.024 084 035 402(72)	−193(130)	1.024 084 035 209(149)
$^{129}Xe^{3+}/^{84}Kr^{2+}$	5	0.976 435 528 013(50)	84(121)	0.976 435 528 096(131)
$^{129}Xe^{3+}/^{12}C^{16}O_2^+$	3	1.023 775 269 022(62)	−297(100)	1.023 775 268 725(118)
$^{84}Kr^{2+}/^{132}Xe^{3+}$	3	1.047 963 133 217(82)	−484(227)	1.047 963 132 733(242)
$^{132}Xe^{3+}/^{12}C^{16}O_2^+$	7	1.000 495 308 740(46)	−157(70)	1.000 495 308 583(84)
$^{86}Kr^{2+}/^{129}Xe^{3+}$	4	1.000 301 596 050(52)	45(64)	1.000 301 596 095(82)
$^{86}Kr^{2+}/^{132}Xe^{3+}$	3	1.023 577 048 954(76)	−112(131)	1.023 577 048 842(151)
$^{132}Xe^{3+}/^{129}Xe^{3+}$	3	0.977 260 673 087(66)	438(98)	0.977 260 673 525(118)

start of the ring-down is larger than ρ_c by the factor $(f_{ct}/f_z)^{1/2}$].

If ε represents the action transfer efficiency of the coupling pulse, we can write $\rho_{c\text{-}res}^2=(1-\varepsilon)\rho_c^2$. Using Eqs. (1) and (2) the perturbation to our value of f_c derived from the "invariance theorem" can then be written

$$\frac{\Delta f_c}{f_c}=[a_0+a_1\varepsilon]\rho_c^2+\left(\frac{f_z}{f_{ct}^2}\right)2\Delta f_z(a_z), \tag{4}$$

where

$$a_0=-\frac{3}{4}\left(\frac{f_z}{f_{ct}}\right)^2\frac{C_4}{d^2}-2\left(\frac{\pi f_{ct}}{c}\right)^2,$$

and

$$a_1=-\frac{1}{2}\frac{B_2}{B_0}+\frac{3}{2}\left(\frac{f_z}{f_{ct}}\right)^2\frac{C_4}{d^2}.$$

In our trap, we can conveniently null C_4 by adjusting the guard-ring voltage. We obtain the correct guard-ring voltage to achieve this, to the level of $|C_4|<10^{-5}$, using a separate procedure wherein we carefully measure f_z of a single ion as a function of magnetron radius ρ_m. However, after our careful magnet shimming with the insert removed, we decided not to reshim the magnet to cancel the B_2 introduced by the diamagnetism of the trap electrodes [19]. To measure B_2 we measured f_{ct} as a function of ρ_c for $^{20}Ne^{2+}$ and $^{20}Ne^{3+}$. For these ions the relativistic and B_2 shifts were comparable in magnitude and opposite in sign. This enabled B_2/B_0 to be determined absolutely using Eq. (1), with only weak dependence on the calibration of the cyclotron drive, with the result $B_2/B_0=-7.9(4)\times10^{-8}$ mm^{-2}. The quantities $(B_2/B_0)\rho_c^2$ for each value of m/q were obtained most accurately, independent of cyclotron drive calibration, by measuring f_z as a function of ρ_c for the different ions whose masses we were measuring. (Combining this with our absolutely measured B_2/B_0 then gave the cyclotron radius calibration, which is only needed to estimate the small relativistic shift.) Unlike C_4, we cannot control the electrostatic anharmonicity C_6. This was measured from the quartic dependence of f_z versus ρ_m and also of f_z versus ρ_c, at large radii. The result was $C_6=1.1(1)\times10^{-3}$, and was found to be constant within the uncertainty. (However, as stated above, since we directly measure $\Delta f_z(a_z)$ as a function of amplitude for the different ions, this value was not needed in our analysis.)

Following Ref. [17], the efficiency for action exchange can be written as

$$\varepsilon=\left[\frac{t'_\pi}{t_\pi}\sin\left(\frac{\pi}{2}\frac{t}{t'_\pi}\right)\right]^2, \tag{5}$$

where t is the actual length of the coupling pulse, t_π is the optimum length (i.e., the pi-pulse time), and t'_π (the optimum length for a finite detuning) is given by $(1/t'_\pi)^2=(1/t_\pi)^2+(2\delta)^2$, where δ is the detuning between the frequency of the coupling drive f_{cc}^{synth} and the optimum value, which is $f_{cc}^{opt}=f_{ct}-f_z$. This detuning resulted from a technical requirement that the synthesizers used for the PNP measurement be set to integer frequencies in order to maintain phase coherence with the computer-generated timing sequence.

Optimally, as was the case for the "doublet" measurements at $m/q=28$ and 32, the cyclotron radii for the two ions being compared are very similar, the pi-pulse efficiencies are close to 1, and the above shifts nearly cancel in the ratio and could be neglected. However, for the ratios involving $^{84,86}Kr^{2+}$ and $^{129,132}Xe^{3+}$ at $m/q=42$ to 44 this was not the case. First, some of the ratios involved a change of m/q. Since in general we kept the cyclotron drive voltage and drive time constant for these measurements, and in our trap the transfer function (the ratio of rf voltage at the trap electrodes to the synthesizer output), has a broad maximum corresponding to $m/q=30$, the change in f_{ct} between these heavier ions led to a few percent change in the cyclotron radius. Second, at these higher values of m/q, because of the lower value of the transfer function, the time required for the cyclotron coupling drive to produce a pi-pulse was as long as 550 ms. This caused a significant sensitivity to cyclotron coupling detuning δ. Finally, it should be noted that systematics for the higher values of m/q are in any case more severe due to the factors of $(f_z/f_{ct})^2$ in Eq. (4).

Using Eqs. (4) and (5), with parameters obtained from the auxiliary measurements of $(B_2/B_0)\rho_c^2$, B_2/B_0, and $\Delta f_z(a_z)$, we obtained amplitude-dependent corrections with estimated uncertainties to be applied to the cyclotron frequency ratios obtained from each run. We then took the weighted average over the runs for a given ratio to determine the correction for each ratio. Depending on the details of the run conditions, these weighted averages showed varying degrees of cancellation. However, in estimating the error in the average correction we combined them linearly, treating them as fully correlated, ignoring possible cancellations. In general, these amplitude-dependent corrections are the largest component of the total systematic corrections shown in Table I. We verified our model for these amplitude-dependent corrections, and checked the uncertainties in the parameters, by carrying out a series of 30 overnight runs with single ions in which the cyclotron radius was systematically varied.

B. Equilibrium position shifts

A difference between the average positions of the two ions whose mass ratio is being measured, combined with a gradient in the magnetic field, leads to a systematic shift in the cyclotron frequency ratio. Such an equilibrium position shift could occur for ions of different m/q, and so ring voltage, due to an offset voltage on the electrodes (such as due to a "charge patch"), that produces an electric field that is not proportional to ring voltage. By systematically biasing the lower end-cap of our trap, and measuring f_c with CH_4^+ and $^{32}S^+$ ions, we measured $B_1/B_0=-4.8(5)\times10^{-8}$ mm^{-1}. By also measuring f_z as a function of lower-end cap bias [13], we determined that any voltage offset was less than 20 mV. Together, these results imply a systematic shift $|\Delta f_c/f_c|<2\times10^{-12}$ in the nondoublet comparisons of $m/q=43$ to 42, and of 43 to 44, implying that this effect can be neglected.

As a check against position-dependent shifts, and in fact all residual shifts that vary as m/q, we compared our corrected cyclotron frequency ratio for $^{40}Ar^+/^{12}C^{16}O_2^+$ (where

m/q changes by 10%) with that obtained from previous mass data [11]. For this we obtained 1.100 782 312 587(90)(450), where we show the statistical uncertainty and estimated uncertainty in the radius-dependent correction separately. This is in good agreement with the value of 1.100 782 312 448(79) obtained from Ref. [11].

C. Coil-pulling shifts

Consideration of the coupling between the ion's axial motion and the coil leads to a shift in the axial frequency, $\Delta f_z = \Delta\omega_z/2\pi$, where

$$\Delta\omega_z = \left(\frac{\gamma_0\gamma_z}{4}\right)\frac{(\omega_z-\omega_0)}{(\omega_z-\omega_0)^2+(\gamma_0/2)^2}, \tag{6}$$

where γ_0 is the width (or damping rate) of the coil resonance, γ_z is the damping rate of the ion on resonance with the coil, and ω_0, ω_z, are the coil resonance and ion axial (angular) frequency, respectively. The interaction of coupled oscillators here, in fact, leads to a pushing of the axial frequency away from the coil frequency. We corrected the measured axial frequency for this effect by using a value for γ_z calculated assuming the usual LC circuit model for the coil and trap. For an ion of mass m and charge q, this gives a damping rate

$$\gamma_z = \frac{Q\omega_0 L}{m}\left(\frac{qC_1}{2z_0}\right)^2 \tag{7}$$

where Q is the quality factor of the coil resonance, L is the coil inductance, $2z_0$ is the minimum separation of the endcaps, and $C_1(\approx 0.8)$, is a factor allowing for the geometry of our trap. Because of uncertainty in the values of L and C_1, we checked the coil-pulling correction by varying $\omega_z-\omega_0$ and observing the effect on our measured cyclotron frequencies (through ω_z). We obtained agreement between the calculated and measured shifts within 30% and thus use this as the uncertainty in this correction. Because we usually adjusted the trap voltages to produce the same f_z for the two ions being compared, this systematic is largest for ions with different charges. For all but one ratio, the average coil-pulling effect was less than 6×10^{-11} and its uncertainty almost negligible. The exception was $^{86}Kr^{2+}/^{132}Xe^{3+}$, for which the coil-pulling correction was $1.26(38)\times10^{-10}$, where we had offset the axial frequency in order to improve the symmetry of the pi-pulse efficiency.

D. Image charge shifts

An additional perturbation to the ion's measured cyclotron frequency is due to the Coulomb interaction between the ion and the image charge it induces in the trap electrodes. A detailed calculation of the shift for the geometry of the MIT trap by Porto [20] gives a shift $\Delta f_c = 91.84(7)$ μHz per electronic charge, independent of mass. The largest image-charge correction, 6.2×10^{-11}, was for $^{132}Xe^{3+}/^{12}C^{16}O_2^+$, with negligible uncertainty.

IV. RESULTS

A. Ion mass ratios

The total systematic corrections to the average cyclotron frequency ratios, due to amplitude-dependent, coil-pulling, and image-charge effects, are listed in the fourth column of Table I. The uncertainty in the total systematic correction was obtained by combining the contributions from the amplitude-dependent and coil-pulling corrections in quadrature.

In the last column of Table I, we show our final results for the corrected cyclotron frequency ratios (inverse ion mass ratios) with combined one-standard-deviation statistical and systematic errors. With the corrections the data show a good degree of self-consistency: all ten triplet comparisons involving Kr and Xe isotopes, such as $(^{86}Kr^{2+}/^{84}Kr^{2+})\times(^{84}Kr^{2+}/^{12}C^{16}O_2^+)/(^{86}Kr^{2+}/^{12}C^{16}O_2^+)$, give unity within errors, for a combined reduced chi-square of 0.16.

B. Atomic masses

To obtain atomic masses from our ion mass ratios we followed the procedure described in [6]. The ion ratios are corrected for the mass of the missing electrons, and for binding energy (using heats of formation and ionization potentials found in Refs. [21–23]), and then converted into an overdetermined set of mass-difference equations. The unknown masses are obtained from a global least-squares fit. For ^{32}S only two ratios are involved and the masses derived from $^{16}O_2^+$ and $^{12}C_2D_4^+$ agreed within the individual errors. For $^{84,86}Kr$, and $^{129,132}Xe$, 12 relevant ratios were included. The fit gave a reduced chi-squared of 0.21, which may indicate that we have overestimated the total errors for the ratios. (In fact a fit to the 12 ratios involving Kr and Xe, without specifying errors on the ratios, gives a set of masses with fractional errors $<4\times10^{-11}$, which agree with our final masses within the final mass errors. However, a fit to the ratios of Table I without the systematic corrections gives a reduced chi-square greater than 10.) The values of the mass of ^{84}Kr derived with respect to $^{14}N_2^+$, $^{40}Ar^+$, and $^{12}C^{16}O_2^+$ all agree within the individual errors, but the doublet determination with respect to $^{14}N_2^+$ is the most precise. These procedures were coded at FSU and were checked by verifying that they reproduced the results of Ref. [6] using the ratios in Ref. [12].

An obvious concern is that correlations in the uncertainties in our mass ratios, stemming from the systematic corrections, could lead to an underestimate of the errors in the masses returned by the global fit. To study this we systematically varied the parameters in the model used to obtain the corrections, then repeated the global fit using the resulting modified ratios. From these systematic shifts we obtained additional contributions to the mass uncertainties of ^{84}Kr, ^{86}Kr, ^{129}Xe, ^{132}Xe of 1.8, 5.5, 5.4, and 2.9×10^{-9} u, respectively, which we combined in quadrature with the errors returned by the global fit. For ^{32}S this led to a negligible increase in the uncertainty. We also note, because our unknown masses are referred primarily to references of the same m/q, or else m/q above and below, they are less sensitive to

TABLE II. Results for the masses of ^{32,33}S, ^{84,86}Kr, and ^{129,132}Xe in atomic mass units (^{12}C=12 u) compared with values from Ref. [11].

Isotope	This work	Audi *et al.* [11]	Difference (10^{-6} u)
^{32}S	31.972 071 173 5(16)	31.972 071 00(15)	0.17(0.15)
^{33}S	32.971 458 908 7(16)	32.971 458 76(15)	0.15(0.15)
^{84}Kr	83.911 497 770 5(50)	83.911 507(3)	−9.2(3.0)
^{86}Kr	85.910 610 672 2(84)	85.910 610 73(11)	−0.058(0.11)
^{129}Xe	128.904 780 960(10)	128.904 779 4(8)	1.56(0.80)
^{132}Xe	131.904 155 190 7(92)	131.904 153 5(10)	1.69(1.00)

m/q-dependent systematic errors than some of the individual ratios.

Table II shows our final results for the masses of ^{32}S, ^{84,86}Kr, and ^{129,132}Xe in atomic mass units, compared with previous values from Ref. [11]. By using the high-precision result for the mass difference $M[^{32}\mathrm{S}]+M[^{1}\mathrm{H}]-M[^{33}\mathrm{S}]=0.008\ 437\ 296\ 82(30)$ u from Ref. [10], and the mass of ^{1}H from Ref. [11], we obtain the mass of ^{33}S. This is also included in Table II. As can be seen, the largest improvement is for ^{84}Kr, where our result, which is 600 times more precise, disagrees with the previous value based on magnetic deflection techniques, by three times the previous quoted uncertainty. By contrast, our result for ^{86}Kr is in good agreement with the previous value obtained using a noncryogenic Penning trap by the Stockholm group [24], and improves the precision by only a factor of 13.

V. CONCLUSION

We have measured the masses of the isotopes ^{32}S, ^{84,86}Kr, and ^{129,132}Xe with relative precisions $\leqslant 10^{-10}$. Together with a new mass for ^{33}S derived using a previously measured mass difference with respect to ^{32}S, these form a significant addition to the table of precision atomic masses [11]. In particular, our measurements of ^{129,132}Xe are measurements at this precision for $A>100$. For Kr and Xe, involving mass comparisons at $m/q\sim 42$, the precision was limited by systematic effects. Of these, the most troublesome were due to variation in the cyclotron radius and cyclotron-to-axial pi-pulse efficiency, combined with trap anharmonicities, particularly those characterized by B_2 and C_6. These effects can be reduced by modifying the cryogenic rf-drive filter electronics to lessen variation in the cyclotron drive radius with frequency, by reshimming the magnet, by modifying the trap electrodes to reduce C_6, and by improving the detector signal-to-noise ratio to allow measurements with a smaller cyclotron radius. The variation in the efficiency of the pi-pulse due to detuning can be reduced by increasing the coupling-drive strength to reduce the pi-pulse time. For an order of magnitude improvement in precision, it will also be necessary to increase the statistical precision. This is limited primarily by instability of the magnetic field, but also by the measurement precision and instability of the ion's axial frequency. As was demonstrated in Ref. [8], both these problems are addressed if the cyclotron frequency comparison can be carried out simultaneously with two ions in the trap.

ACKNOWLEDGMENTS

We acknowledge D. E. Pritchard, S. Rainville, and J. K. Thompson for generously enabling the relocation of the Penning trap system and sharing their expertise; and W. W. Brey (NHMFL) for assistance with magnet shimming and loan of equipment. The participation of J. Victoria, M. Wierman (REU), and of J. Malmaud, N. Horton (Young Scholar Program), and the technical assistance of K. Koetz and G. Brown, are also acknowledged. This work was supported by NSF Contract No. PHY-0354741 and by the State of Florida.

[1] E. A. Cornell, R. M. Weisskoff, K. R. Boyce, R. W. Flanagan, Jr., G. P. Lafyatis, and D. E. Pritchard, Phys. Rev. Lett. **63**, 1674 (1989).
[2] R. S. Van Dyck, Jr., D. L. Farnham, and P. B. Schwinberg, Phys. Rev. Lett. **70**, 2888 (1993).
[3] G. Gabrielse, A. Khabbaz, D. S. Hall, C. Heimann, H. Kalinowsky, and W. Jhe, Phys. Rev. Lett. **82**, 3198 (1999).
[4] R. S. Van Dyck, Jr., S. L. Zafonte, and P. B. Schwinberg, Hyperfine Interact. **132**, 163 (2001).
[5] R. S. Van Dyck, Jr., S. L. Zafonte, S. Van Liew, D. B. Pinegar, and P. B. Schwinberg, Phys. Rev. Lett. **92**, 220802 (2004).
[6] F. DiFilippo, V. Natarajan, K. R. Boyce, and D. E. Pritchard, Phys. Rev. Lett. **73**, 1481 (1994).
[7] M. P. Bradley, J. V. Porto, S. Rainville, J. K. Thompson, and D. E. Pritchard, Phys. Rev. Lett. **83**, 4510 (1999).
[8] S. Rainville, J. K. Thompson, and D. E. Pritchard, Science **303**, 334 (2004).
[9] J. K. Thompson, S. Rainville, and D. E. Pritchard, Nature (London) **430**, 58 (2004).
[10] S. Rainville *et al.* (unpublished).

[11] G. Audi, A. H. Wapstra, and C. Thibault, Nucl. Phys. **A729**, 337 (2003).
[12] F. DiFilippo, Ph.D. Thesis, MIT, 1994.
[13] M. P. Bradley, Ph.D. Thesis, MIT, 2000.
[14] S. Rainville, Ph.D. Thesis, MIT, 2003.
[15] J. K. Thompson, Ph.D. Thesis, MIT, 2003.
[16] L. S. Brown and G. Gabrielse, Rev. Mod. Phys. **58**, 233 (1986).
[17] E. A. Cornell, R. M. Weisskoff, K. R. Boyce, and D. E. Pritchard, Phys. Rev. A **41**, 312 (1990).
[18] The weights used to average the different runs for the same ratio are $1/(\sigma(i)^2_{stat}+\sigma(i)^2_{syst})$, where $\sigma(i)_{stat}$ and $\sigma(i)_{syst}$ are the statistical and systematic uncertainties, respectively, for each run.
[19] Reshimming the magnet to compensate for the trap diamagnetism causes the magnetic field at the trap center to be sensitive to motion of the trap with respect to the magnet. An alternative is to apply ferroshims directly to the trap housing.
[20] J. V. Porto, Phys. Rev. A **64**, 023403 (2001).
[21] M. W. Chase, J. Phys. Chem. Ref. Data **9**, 1 (1998).
[22] NIST Chemistry WebBook, edited by P. J. Linstrom and W. G. Mallard, http://webbook.nist.gov
[23] Y. H. Le Teuff, T. J. Millar, and A. J. Markwick, Astron. Astrophys., Suppl. Ser. **146**, 157 (2000).
[24] T. Fritioff and G. Douysset, Phys. Scr. **67**, 276 (2003).